Composites Science and Technology 230 (2022) 109740

Contents lists available at ScienceDirect

Composites Science and Technology

journal homepage: www.elsevier.com/locate/compscitech

Mechanically robust, stretchable, recyclable, and biodegradable ionogels reinforced by polylactide stereocomplex nanocrystals

Haopeng Zhang [a], Xiaohui Yu [a], Yufei Wang [a], Xiaoshan Fan [a,*], Yue-E Miao [a], Xu Zhang [b,**], Tianxi Liu [a,b,***]

[a] State Key Laboratory for Modification of Chemical Fibers and Polymer Materials, College of Materials Science and Engineering, Donghua University, Shanghai, 201620, People's Republic of China

[b] Key Laboratory of Synthetic and Biological Colloids, Ministry of Education, School of Chemical and Material Engineering, International Joint Research Laboratory for Nano Energy Composites, Jiangnan University, Wuxi, Jiangsu, 214122, People's Republic of China

ARTICLE INFO

Keywords:
Ionogels
Stereocomplex nanocrystallites
Recyclability
Biodegradability
Flexible wearable sensors

ABSTRACT

Spider silk possesses the combined properties of high strength, great toughness, and good elasticity due to the unique two-phase structures, in which the β-sheet nanocrystals consisting of hydrogen-bonded polypeptide chains are connected by the flexible chains. The spider-silk-like structures provide novel avenues to create functional materials. Herein, a novel yet simple strategy has been developed for the fabrication of spider-silk-like ionogels. The scaffolds of ionogels, polyurethane (scPLA-PEG), were prepared from poly(L-lactide) (PLLA), poly (D-lactide) (PDLA), and poly(ethylene glycol) (PEG). The stereocomplex nanocrystallites (sc) could be formed through the multiple hydrogen-bonds on the enantiomeric PLLA and PDLA chains, thus the as-prepared scPLA-PEG possesses the spider-silk-like two-phase structures, in which the stereocomplex nanocrystallites are cross-linked by the amorphous PEG phases. As compared, the scPLA-PEG exhibit much higher mechanical properties than the pristine PLA counterparts. The scPLA-PEG ionogels also display good mechanical properties, extremely temperature-tolerant flexibility that endures twisting at low temperature (−30 °C) and stretching at high temperature (70 °C). Furthermore, the scPLA-PEG ionogels can be easily recycled owning to the reversible properties of scPLA. The results would present a new insight into designing novel functional ionogels with distinguished mechanical properties, tractable recyclability, and biodegradability, which will promote the sustainable flexible electronics.

1. Introduction

In nature, many biological tissues and materials have developed miraculous noncovalent self-assemblies of biomacromolecules, which exhibit an extraordinary combination of remarkable mechanical properties [1]. The outstanding example is spider silk, which is one of the most robust natural materials and has extremely high strength, excellent toughness, and good elasticity [2,3]. Spider silk possesses a unique two-phase structure, in which the β-sheet nanocrystals consisting of hydrogen-bonded (H-bonded) polypeptide chains, are connected by flexible chains [3]. Moreover, it has been experimentally and theoretically proved that the remarkable strength and toughness of spider silk are attributed to the unique H-bond arrays in the β-sheet nanocrystals [4]. So, the biomolecular system of spider-silk-like showcased here provides the novel avenues to create materials with significantly improved mechanical properties. In recent years, a few high-performance synthetic materials have been developed by rationally designing the cross-linked networks via the higher density of H-bond arrays [5–8]. However, the fabrication of these materials by mimicking the spider silk still remains a long-standing challenge, which involves tedious multistep processes for the construction of spider-silk-like β-sheet nanocrystal networks and is not suitable for large-scale production in the practical applications [9,10].

Ionogels [11,12], defined as the polymeric networks filled with ionic

* Corresponding author.
** Corresponding author.
*** Corresponding author. State Key Laboratory for Modification of Chemical Fibers and Polymer Materials, College of Materials Science and Engineering, Donghua University, Shanghai, 201620, People's Republic of China.
E-mail addresses: xsfan@dhu.edu.cn (X. Fan), xuzhang@jiangnan.edu.cn (X. Zhang), txliu@jingnan.edu.cn (T. Liu).

https://doi.org/10.1016/j.compscitech.2022.109740
Received 15 August 2022; Received in revised form 8 September 2022; Accepted 13 September 2022
Available online 17 September 2022

liquids (ILs), have been garnering great interesting as the promising soft electrolytes for applications in flexible sensors [13–17], owning to their unique characteristics attributed to the intrinsic properties of the ILs [18,19]. Generally, the ionogel networks are generally needed to be covalently cross-linked to acquire the high elasticity and chemical resistance [20–22]. However, the irreversible covalent cross-linking makes the cross-linked ionogels be incapable of recycling and processing after finishing the corresponding tasks. Alternatively, incorporating noncovalent bonds or dynamic covalent bonds into polymer networks has been proposed to fabricate recyclable and reprocessable ionogels with high elasticity and mechanical robustness [23–29]. The incorporation of these reversible bonds empowers the formed networks with recyclable and reprocessable properties [30,31]. Despite the burgeoning progress achieved so far, the existing ionogels mostly employ nondegradable materials as the network scaffolds (such as silicone or acrylic elastomers (poly(n-butyl acrylate) (PnBA), VHB), which might cause secondary environmental pollution at the end of their functional life [32–35]. Currently, the ionogels based on biodegradable and eco-friendly materials are extremely rare. So, it is highly desirable to develop recyclable and reprocessable ionogels with biodegradable properties, which can contribute to build a sustainable society by extending the service life of the materials and reducing the resource waste and environmental pollution.

In this contribution, a novel yet simple strategy has been developed for the fabrication of recyclable and biodegradable ionogels with high performance, which features the unique two-phase structures similar to spider silk. As illustrated in Fig. 1, the polyurethane scPLA-PEG was first synthesized from poly(L-lactide) (PLLA), poly(D-lactide) (PDLA), and poly(ethylene glycol) (PEG) in a "two-step one-pot" reaction (Fig. 1a). Among them, the PLLA and PDLA two enantiomers can form the stereocomplex nanocrystallites (sc) through the multiple hydrogen-bonds on the enantiomeric chains. So, the as-prepared scPLA-PEG possesses the unique spider-silk-like two-phase structures, in which the scPLA nanocrystallites are connected by the flexible PEG chains (Fig. 1b). The comparative study of the as-prepared scPLA-PEG was conducted with the corresponding counterparts and the scPLA-PEG ionogels displayed much higher mechanical properties with the breaking tensile strain, stress, and Young's modulus up to 1460%, 6 MPa, and 3.5 MPa, respectively. The notable improved mechanical properties should be contributed to the spider-silk-like structures. Additionally, the scPLA-PEG ionogels exhibited the integrated advantages such as biodegradability, recyclability, mechanical robustness, and high stretchability, benefiting from the reversible and biodegradable properties of the "sc" cross-linking.

2. Experimental methods

2.1. Materials

The L-lactide (L-LA) and D-lactide (D-LA) were purchased from Shenzhen Match Biomaterials Co. and used as received. The polyethylene glycol (PEG-1K, M_n = 1000 g/mol), 1,4-butanediol (BDO, > 98%), ethylene glycol (EG, > 99.5%), 1-butyl-3-methylimidazolium tetrafluoroborate ([EMIM][BF4], 99%), anhydrous tetrahydrofuran (THF, > 99.5%), anhydrous toluene (>99.5%) were purchased from Shanghai Titan Scientific Co. The stannous octoate ($Sn(Oct)_2$, 95%) was purchased from Sigma-Aldrich (Shanghai, China). The 1,6-hexamethylene diisocyanate (HDI, 99%) was purchased from Shanghai Yien Chemical Technology Co. The dibutyltin dilaurate (DBTDL, 95%) was purchased from Sigma-Aldrich (Shanghai, China). The BDO was stored with the presence of 4 Å molecular sieves. The THF and toluene were dried using a solvent purification system. The VHB tapes were purchased from Minnesota Mining and Manufacturing (3M) Co.

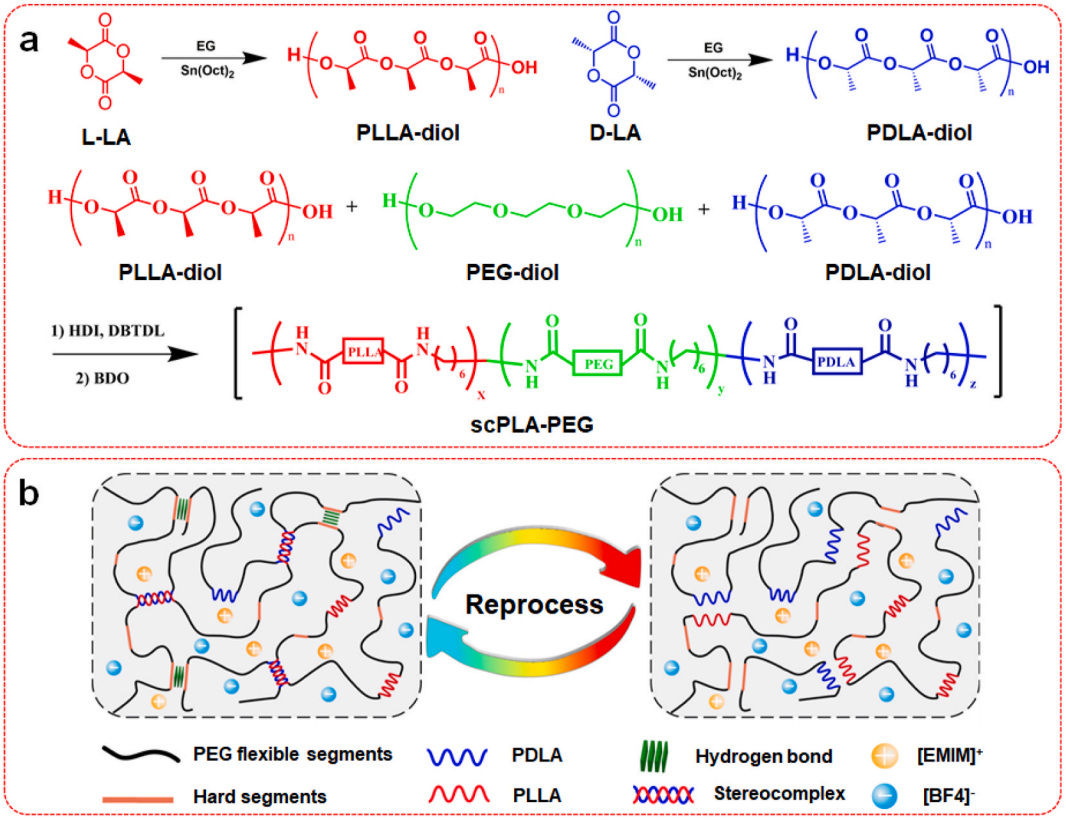

Fig. 1. (a) Chemical structure of the PLA-diol, PEG-diol, PDLA-diol, and scPLA-PEG polyurethane. (b) Schematic structure of the scPLA-PEG based ionogels with 30% ionic liquids (scPLA-PEG/30%-ILs).

2.2. Synthesis of PLLA and PDLA macrodiols

The PLLA-diol and PDLA-diol were synthesized through the ring opening polymerization. In a typical procedure, the 15 g of L-lactide monomer and 90 μL of $Sn(Oct)_2$ were heated at 90 °C in a 250 mL round-bottomed flask equipped with a magnetic stirrer under vacuum and stirred for 0.5 h to remove water. Then, 275 μL EG and 50 mL anhydrous toluene were added into the reactants under nitrogen atmosphere, and the reactants were stirred at 130 °C for 24 h. The products were precipitated, washed with ether, and dried at 40 °C in a vacuum oven for 12 h. The molecular weight of the PLLA-diol and PDLA-diol were characterized by GPC (PLLA: $M_{n,\ GPC} = 3730$ g/mol, PDI = 1.11; PDLA: $M_{n,\ GPC} = 4020$ g/mol, PDI = 1.16).

2.3. Preparation of scPLA-PEG polyurethane

In a typical procedure, the 8g PEG (8.00 mmol), 1g PLLA-diol (0.27 mmol), 1g PDLA-diol (0.25 mmol), and two drops of catalyst DBTDL were heated at 100 °C in a 100 mL round-bottomed glass flask under vacuum and stirred for 1 h to remove water. Then, the mixture was cooled down to 60 °C, and then the 1.72 g HDI (10.22 mmol) and 40 mL THF were added to the flask under nitrogen atmosphere for 2 h. After that, 0.15 g BDO (1.7 mmol) were added into the reaction solution and the reaction continued until the NCO peak in the FT-IR spectrum disappears ($M_{n,\ GPC}$ = 20,000 g/mol, PDI = 1.18). For comparison, three other polyurethanes, denoted as PLLA-PEG, PDLA-PEG, and PEG-PEG, were also synthesized according to the same way.

2.4. Preparation of polyurethane ionogels

The THF solutions of polyurethane (PU) networks were mixed with the ionic liquids [EMIM][BF4] in different mass ratios in a glass bottle under vigorously stirring. Then, the mixture solutions were poured into a Teflon dish, and the solvents were evaporated for 12 h in an oven at room temperature to provide the ionogels. Finally, the samples were completely dried at 50 °C under vacuum for 12 h. Four samples of the scPLA-PEG based ionogels with different contents of ILs were fabricated, which were denoted as scPLA-PEG/0%-ILs, scPLA-PEG/20%-ILs, scPLA-PEG/30%-ILs, scPLA-PEG/40%-ILs, respectively.

2.5. Characterization

The HNMR spectra of the scPLA-PEG were performed on an AVANCE III 600 MHz NMR spectrometer using $CDCl_3$ as the solvents. The attenuated total reflection Fourier transform infrared (ATR-FTIR) spectra were carried out on a Nicolet IS50 infrared spectrophotometer in the range of 4000-525 cm^{-1}. The X-ray diffraction (XRD, D8 Advanced, Bruker) patterns used the Cu K_α radiation from 5° to 40° at a scanning rate of 5° min^{-1}. The differential scanning calorimetry (DSC) measurements were measured on a TA Q2000 from −70 °C to 240 °C at a heating/cooling rate of 10 °C min^{-1} under the nitrogen atmosphere. The thermal gravimetric analysis (TGA) tests were performed on a TG 209 F1 from room temperature to 600 °C in the N_2 atmosphere with the heating rate of 10 °C min^{-1}. The rheological measurements were characterized by an Anton Paar MCR302 rheometer using a 25 mm parallel plate geometry. The strain sweep tests were performed at the shear strain from 0% to 100% at a constant angular frequency of 5 rad s^{-1}. The frequency ranges from 0.1 rad s^{-1} to 300 rad s^{-1}. The gel permeation chromatographic (GPC) measurements were conducted using the 1260 Infinity II system, equipped with two Phenomenex linear 5 mm Styragel columns, and the THF were used as the eluent at the flow rate of 1.0 mL min^{-1}. The mechanical properties of the samples were measured by a universal testing machine (SUNS, Shenzhen, China).

The conductivity (σ) was calculated bywhere R, L, and A represents the resistance, length, and cross-sectional area of ionogel samples, respectively. The Young's moduli were calculated from the initial slope linear stage of the stress-strain curves, and the toughness values were calculated by integrating the area under the stress-strain curves. The cyclic tensile tests were performed for 10 times under the tensile speed of 30 mm min^{-1}. The digital images were captured using a Nikon D5100 camera.

The $\Delta R/R_0$ and GF value are calculated by the following formulas, respectively,

$$\frac{\Delta R}{R_0} = \frac{R - R_0}{R_0}$$

$$GF = \frac{\Delta R/R_0}{\varepsilon}$$

where R and R_0 are the real-time and initial resistances, respectively. ε is the applied strain.

The resistance from the resistive-type strain sensor was measured on a Keithley 2616 System source meter at a voltage of 5 V. The resistive-type strain sensing device was assembled with two copper foil current collectors sandwiched with an ionogel sample, and the copper foil current collectors were used for connecting the testing wires.

Small Angle X-ray Scattering (SAXS) scattering patterns were measured using a SAXSess MC^2 system in line collimation, operated at 40 kV and 50 mA producing Cu K_α radiation (X = 1.5418 A). Data were collected for 20 min. The interdomain spacing (d) was calculated by Bragg's equation:

$$d = \frac{2\pi}{q_{max}}$$

where q_{max} corresponds to the peak position of one-dimensional SAXS curve.

Dynamic light scattering (DLS) was utilized to measure the apparent hydrodynamic radius of related polymers, at 25 °C with a Brookhaven BI-200SM multiangle goniometer equipped with a Brookhaven BI-APD avalanche photodiode detector.

The crystallinity of PLA was calculated according to the equation:

$$Xc = \frac{\Delta H_m}{\Delta H_m^{100}} \times 100\%$$

where ΔH_m is the experimental melting enthalpy of a fraction, determined as the integral intensity of the melting peak. ΔH_m^{100} is the specific melting enthalpy of 100% crystalline polymer, which is 142 J g^{-1} for the PLA stereocomplex crystalline and 100 J g^{-1} for the PLA homogeneous crystalline.

3. Results and discussion

It has been reported that the two enantiomers of biodegradable PLA, referring to PLLA and PDLA, could form stereocomplexes through multiple hydrogen-bonding interactions between the two enantiomeric chains, which could provide the promising physical cross-linking to reliably fabricate the reinforced materials with favorable mechanical properties [36–38]. According to the synthetic routes depicted in Fig. 1, we exploited the tendency of PLLA and PDLA for stereocomplexation to reliably generate the physical cross-linking for fabricating the high-performance ionogels. First, the PDLA-diol and PLLA-diol were synthesized by the ring-open polymerization method using ethylene glycol (EG) as the initiators and stannous octoate $Sn(Oct)_2$ as the catalysts. Then, the poly(PLLA/PEG/PDLA urethane) (denoted by scPLA-PEG) ionogels were prepared via the "two-step one-pot" method. The pre-polymers were synthesized through the condensation reaction between PLLA, PDLA, and PEG with 1,6-hexamethylene diisocyanate (HDI). The scPLA-PEG polyurethanes were obtained by the chain extension reaction using 1,4-butanediol (BDO) as the chain extenders. Introducing the ionic liquids (ILs) into the scPLA-PEG networks to provide the ionogels with spider-silk-like structures, in which the hard

sc-phases as the dynamic cross-linking are homogeneously embedded in the soft continuous PEG phases.

The as-prepared scPLA-PEG polyurethanes and their precursors were well characterized by several technologies. Figs. S1a and S1b respectively show the ^{1}H NMR spectra of the PLLA and PDLA macrodiols, in which the methine proton (-COC***H***(CH_3)-) and methane protons (-COCH(C***H***$_3$)-) signals for PLA block can be seen clearly [39,40]. As compared, the signals assigned to PLA and PEG blocks appear apparently in the ^{1}H NMR spectrum of the scPLA-PEG (Fig. S1c), demonstrating the successful synthesis of the scPLA-PEG elastomers. Meanwhile, the GPC trace of the obtained scPLA-PEG obviously shifts toward the higher molecular region (Fig. S2), further confirming the successful fabrication of the scPLA-PEG. Moreover, the peaks at 1535 cm^{-1} and 3350 cm^{-1} can be seen clearly, which are ascribed to the characteristic stretching vibration and bending vibration of –NH– bond on –NHC(O)O groups, respectively, indicating the coupling reaction proceeded successfully (Fig. S8). Upon mixed together, the stereocomplexation between PLLA and PDLA segments takes place. The PLA stereocomplexes in the scPLA-PEG networks were investigated by XRD and DSC. As shown in Fig. S3a, the characteristic diffraction of the stereocomplex crystallites at around 2θ = 11.8°, 20.6°, and 23.8° were observed clearly in the scPLA-PEG, which assigns to the unique reflection of 110, 300/030, and 220 plane of the stereocomplex crystallites, respectively [41,42]. In the controlled samples of poly(PLLA/PEG urethane), poly(PDLA/PEG urethane), and poly (PEG urethane) (denoted by PLLA-PEG, PDLA-PEG, PEG-PEG, respectively), the diffraction peaks attributed to the typical lattice planes of the PLA homocrystallites are very weak, and these might be affected by the presence of the PEG segments. Moreover, there are obvious diffraction peaks attributed to the stereocomplex crystallites event in the formed ionogels from the scPLA-PEG polyurethanes (scPLA-PEG/ILs), indicating the strong interactions and good stability of the stereocomplex crystallites. The results of DSC (Fig. S3b) are consistent with those of the XRD, and the intensity of the characteristic peak of the PLA stereocomplex crystallites in the scPLA-PEG is much stronger than those of the PLA homocrystallites in PLLA-PEG and PDLA-PEG, further confirming the formation of stereocomplex crystallites in the scPLA-PEG. Generally, the T_m of the stereocomplex and homogeneous crystallites is greater than 200 °C and less than 180 °C, respectively [43]. However, the T_m of the stereocomplex crystallites in the scPLA-PEG is between 180 °C and 200 °C, while such lowering of the T_m should correspond to the small crystallites derived from multiblock copolymers with shorter PLA sequences [44]. The nanostructures of the scPLA-PEG elastomers were further studied by the small-angle X-ray scattering (SAXS), and the size of sc crystals is about 16 nm calculated according to SAXS profiles. These results indicate that the scPLA-PEG elastomer possesses a spider-silk-like two-phase structure with scPLA nanocrystals composed of hydrogen bonds uniformly distributed in the amorphous PEG.

Owing to the spider-silk-like structures, the as-fabricated scPLA-PEG polyurethanes were expected to exhibit the good mechanical properties. Accordingly, the as-prepared elastomers exhibit great stretchability (elongation at break approaches to 1500%), as the direct insights shown in Fig. 3a. In order to systematically investigate the effect of the sc-interactions on the mechanical properties of the as-prepared polyurethane, a series of tests have been conducted. First, the tensile tests were performed to compare the mechanical properties of the scPLA-PEG with PLLA-PEG, PDLA-PEG, and PEG-PEG. From Fig. 2b–c and Fig. S4, it can be seen that the Young's modulus, tensile strength, elongation at break, and toughness of the scPLA-PEG are much higher than those of the controlled samples (PLLA-PEG, PDLA-PEG, and PEG-PEG). Meanwhile, the sc presence in the polymer networks impart scPLA-PEG elastomers with good thermal stability than the precursors PLLA-diol and PDLA-diol, as shown in Fig. S10. The relative strong sc-interactions in the scPLA-PEG networks account for the superior mechanical properties. Subsequently, to further evaluate the elasticity of the scPLA-PEG, the cyclic tensile loading-unloading tests without waiting time between two consecutive loading cycles were carried out with the strain ranging from 100% to 500%. Fig. 2d shows that the scPLA-PEG could nearly recover to the original state after the first tensile cycle with 100% strain and the good elasticity probably originates from the fracture of the stereocomplex crystallites during the stretching process. Meanwhile, the

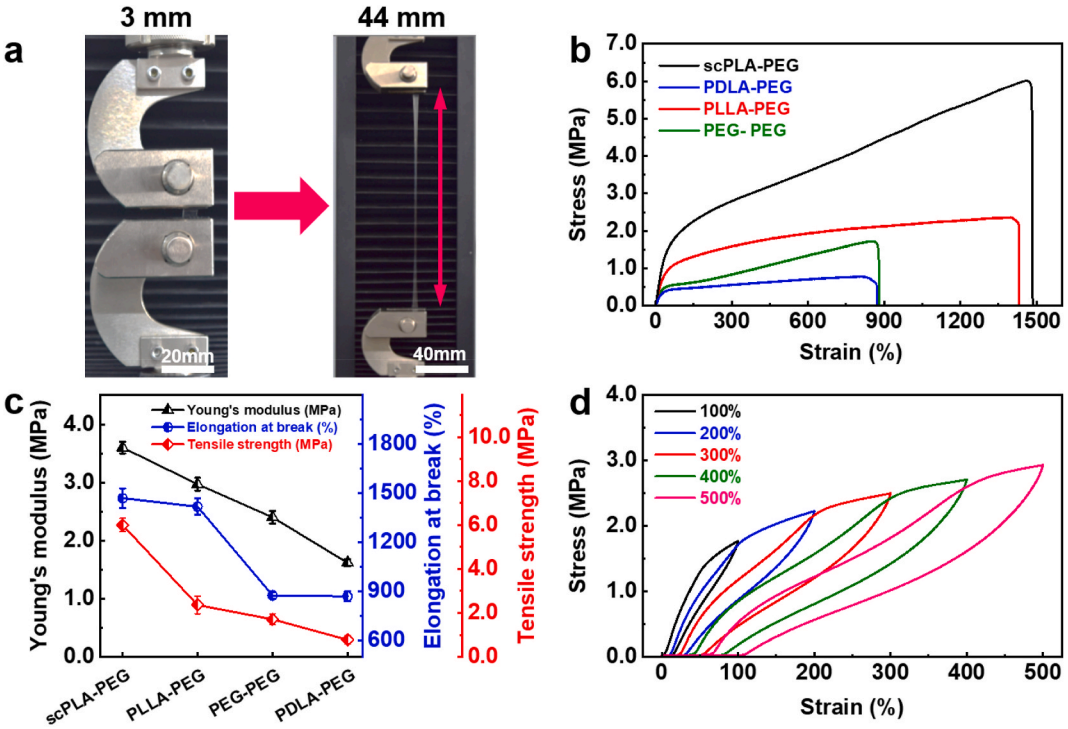

Fig. 2. (a) Photographs of the scPLA-PEG film before and upon stretching. (b) Stress-strain curves of the scPLA-PEG, PDLA-PEG, PLLA-PEG, and PEG-PEG. (c) The elongation at break, Young's modulus, and tensile strength of the scPLA-PEG, PLLA-PEG, PDLA-PEG, and PEG-PEG. (d) Sequential cyclic tensile curves of the scPLA-PEG at different strains without waiting time between two consecutive loadings.

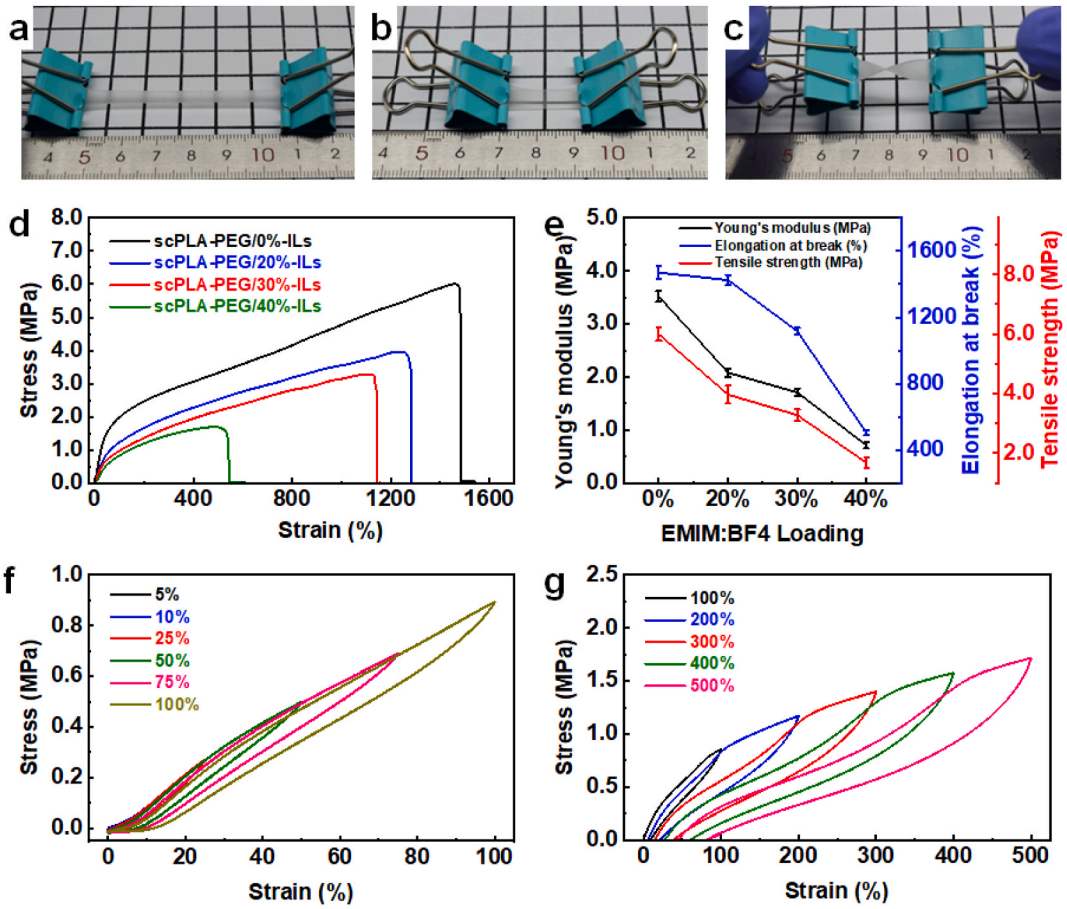

Fig. 3. Photos of the scPLA-PEG/30%-ILs in (a) stretched, (b) relaxed, and (c) twisted states. (d) The stress-strain curves of scPLA-PEG ionogels with different loadings of ILs. (e) Dependences of the elongation at break, Young's modulus, and tensile strength of the scPLA-PEG ionogels on the EMIM:BF4 loading. The stress-strain curves of the scPLA-PEG/30%-ILs ionogels under (f) smaller (0–100%) and (g) larger (100%–500%) maximum strain without waiting time between two consecutive loadings.

obvious hysteresis loops were observed after sequential cycles with higher strains and the hysteresis loop area increases as the strain increases, which might be contributed to the deformation of the dynamic physical cross-linking stereocomplex crystallites. Additionally, the pronounced hysteresis at very strain implied the efficient energy dissipation during the stretching-releasing process [45,46].

Introducing the ionic liquids (ILs) into the as-fabricated scPLA-PEG networks to produce the ionogels and the results aforementioned have indicated that the introduction of ILs would not disturb the physical cross-linking stereocomplex crystallites (as demonstrated in Fig. S3a). So, the as-formed ionogels (scPLA-PEG/ILs) should also possess the excellent mechanical properties. As shown in Fig. 3a–c, the ionogels can be twisted or stretched repeatedly, demonstrating they have the good flexibility and stretchability. The impact of the IL contents on the mechanical properties of the ionogels was also investigated and it was observed that the Young's modulus, elongation and stress at break of the ionogels gradually decreases with the increase in the IL content from 0% to 40% (Fig. 3d and e). The decreased mechanical properties might be attributed to the plasticization effect of the ILs. Considering the combination of conductivity and mechanical properties of the ionogels, the samples scPLA-PEG/30%-ILs (scPLA-PEG with 30% ILs) were selected as the optimal samples for the following measurements unless otherwise mentioned. Subsequently, the cyclic tensile tests with different strains without waiting time between two consecutive loadings were conducted to study the toughness and elastic properties of the scPLA-PEG/30%-ILs. Fig. 3f shows that the ionogels could nearly recover to the original state in every cycle during the small strain (5%–100%), implying that the ionogels possess the excellent elasticity within the 100% strain feasible for most of the practical applications [47,48]. By contrast, the larger hysteresis loops were observed as the maximum strain increases from 100% to 500%, due to the dissociation of the sc-interactions during the deformation process. Importantly, the scPLA-PEG/30%-ILs ionogels displayed the good electrical conductivity while maintaining better mechanical properties, where the electrical conductivity and toughness is up to 3.5×10^{-2} S m^{-1} (Fig. S5a) and 25.4 MJ m^{-3} (Fig. S5b), respectively.

The dynamic rheological tests were carried out to further study the rheological behaviors and thermal stability of the as-prepared ionogels. Shown in Fig. 4a is the oscillatory amplitude sweeps of the scPLA-PEG/30%-ILs. Within a wide strain range, the storage modulus (G') of the scPLA-PEG/30%-ILs is much higher than the loss modulus (G''), assuming the solid elastic properties. As the shear strain increases, the G' and G'' decreases simultaneously, while the decrease rate of the G' shows greater than that of the G''. With further increasing the shear strain beyond the intersection point (Strain ≈50%), the G'' become higher than the G', indicating that the physically cross-linked networks are damaged under relatively larger shear strain. In addition to the amplitude, the oscillation frequency sweeps were also performed under small shear strain (0.1%) (Fig. 4b), the G' and G'' exhibit a strong dependence on the angular frequency, where the G' always exceeds the G'' in the whole angular frequency sweep range, indicating the stability of the physically cross-linked networks. Not only that, the G' is much larger than the G'' at 5 °C, 5–70 °C, and 70 °C (Fig. 4c), indicating that the as-prepared ionogels possess the good stability during a broad temperature ranging

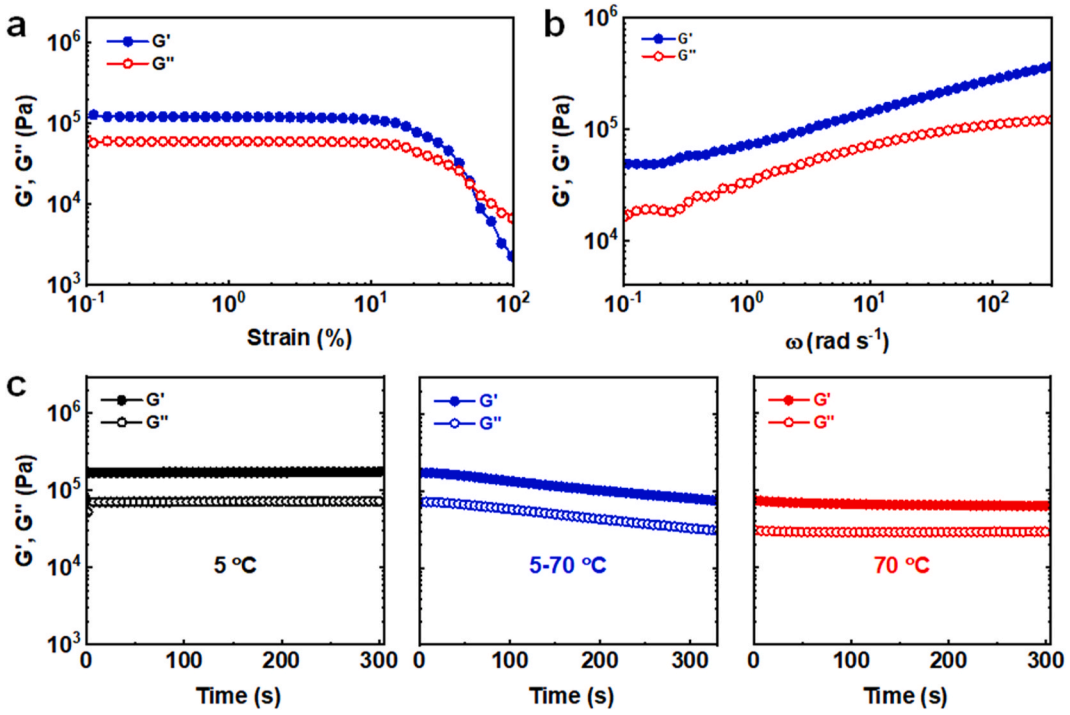

Fig. 4. Oscillatory (a) amplitude sweeps from 0.1% to 100% and (b) frequency sweeps at 0.1% maximum shear strain for the scPLA-PEG/30%-ILs. (c) Storage and loss modulus of the scPLA-PEG/30%-ILs in the temperature ranging from 5 to 70 °C.

from 5 to 70 °C.

Owing to the low freezing point of the ionic liquids ([EMIM][BF4]), the ionogels should maintain the good stretchability under low temperature. In order to demonstrate the anti-freezing performance of the scPLA-PEG ionogels, the DSC analysis was employed to measure the T_g, as presented in Fig. 5a. The DSC results show that the T_g of the ionogels with various IL contents is ca. −47.8 °C, indicating that the scPLA-PEG ionogels could maintain the high elasticity at critical low temperature ($> T_g = -47.8$ °C), which are able to fully meet the main requirements of the scPLA-PEG ionogels to work below zero temperature. Besides the lowest temperature based on T_g, the highest temperature of the high elasticity of the scPLA-PEG ionogels corresponding to the sol-gel transition temperature ($T_{sol\text{-}gel}$) could be exactly obtained from the variation in the storage and loss modulus as a function of temperature, which is found to be ca. 96 °C as resulted in Fig. 5b. Note that the ionogels are capable of sustaining the stable gel networks below $T_{sol\text{-}gel}$. Namely, the high elasticity of the scPLA-PEG ionogels could be remained in a wide temperature range between T_g and $T_{sol\text{-}gel}$ ($T_g < T < T_{sol\text{-}gel}$). Taking the

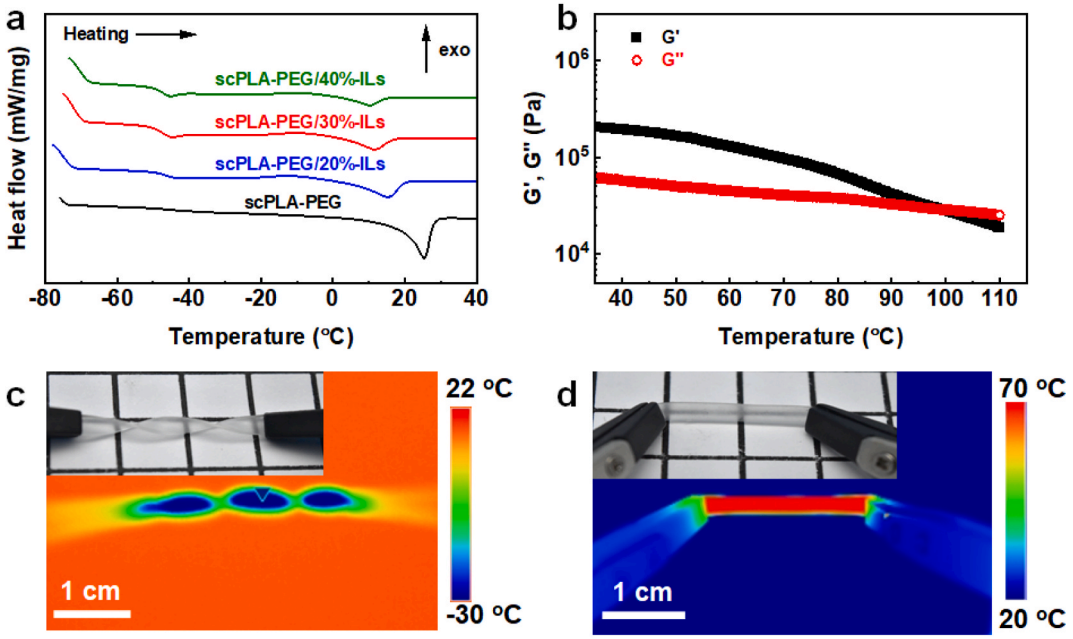

Fig. 5. (a) DSC thermograms of the scPLA-PEG ionogels from −80 °C to 40 °C. (b) Variation in the storage and loss modulus of the scPLA-PEG/30%-ILs as a function of temperature. Photographs and infrared images of the scPLA-PEG/30%-ILs (c) twisted at −30 °C and (d) stretched at 70 °C.

scPLA-PEG/30%-ILs as an example, Fig. 5c and d illustrates that the ionogels could be twisted at −30 °C (> T_g = −47.8 °C) and stretched at 70 °C (<$T_{sol\text{-}gel}$ = 96 °C), indicating that the as-prepared scPLA-PEG ionogels are able to be flexible under extreme temperature conditions.

Thanks to the physically cross-linked networks via the sc-interactions between PDLA and PLLA segments in the scPLA-PEG polymer chains, the scPLA-PEG ionogels would also possess the excellent recyclable performance. Here, the reprocessing ability of the scPLA-PEG ionogels was firstly demonstrated by a simple cutting-thermocompression process, in which the bulk sample was cut into small pieces and then hot-pressed at 96 °C for 0.5 h under a pressure of 2 MPa, as schemed in Fig. S6. Moreover, the scPLA-PEG ionogels could also be dissolved and recycled at room temperature due to the noncovalently cross-linked structures. The scPLA-PEG/30%-ILs samples appeared to dissolve in THF after 1 h at room temperature, as shown in Fig. 6a. After removing the THF, the scPLA-PEG ionogels were reprocessed into a smooth and homogenous film, and the process can be repeated multiple times. In comparison, the recycling process is simple and practicable, which does not require the addition of other chemical and/or higher temperature. Moreover, the reprocessed scPLA-PEG ionogel samples via thermal-process show the obviously decreased mechanical properties in comparison with that recycled via solvent-process because of the insufficient exchange of stereocomplex units (Fig. 6b). Fig. 6c shows the tensile curves of the solvent-recycled scPLA-PEG ionogels and it can be observed that the samples could nearly recover to the original breaking elongation after three cycles of the repeated cycling processes [49]. Most importantly, their recovery ratios of Young's modulus were all more than 90%, and all of these results aforementioned confirmed that the scPLA-PEG ionogels with superior mechanical properties and extraordinary recyclability were achieved (Fig. 6d).

The combination of the excellent mechanical properties and good electrical conductivity makes the as-prepared scPLA-PEG ionogels the ideal promising flexible conductors for the assembly of the wearable electronic sensors. First, the flexible sensors were integrated by sandwiching the scPLA-PEG/30%-ILs with two pieces of VHB (see Fig. S7 in the Supporting Information) [50], which are able to monitor the external mechanical stimuli (such as stretching and bending, etc.) by converting them into the electrical signals. Meanwhile, due to the unique sandwich structure, the formed sensors displayed insensitivity to humidity, as shown in Fig. S11. The relative resistance changes ($\Delta R/R_0$) of the as-fabricated ionogel sensors with regard to applied tensile strain ranging from 0 to 300% (Fig. 7a). The calculated gauge factor (GF) was 1.15 during the stain range of 0–200%, while reached to 1.24 (200–300%) as the applied stain increasing from 200% to 300%, implying that the ionogel sensors have the high strain sensitivity. The relative resistance changes ($\Delta R/R_0$) of the sensors under small (5%, 10%, and 20%) and large (100%, 200%, and 300%) strain were further presented in Fig. 7b and c, respectively. The good repeatability and recognition of the strain sensitivity were clearly observed, which proves the stability of the as-fabricated flexible strain sensors. In addition, for the stretching rate, the $\Delta R/R_0$ rapidly changes as the stretching rate varies from 50 mm min^{-1} to 100 mm min^{-1} and then to 150 mm min^{-1} (Fig. 7d), indicating that the sensors could make a good match between the mechanical and the electrical signals. Moreover, the signals keep stable and reproducible under 300 cyclic tensile tests at 50% strain (Fig. 7e), showing the excellent reliability of the scPLA-PEG ionogels during the long-term cycles. Depending on the remarkable sensing performance, the as-fabricated sensors were directly attached onto diverse joints (elbow and finger) of the puppet for monitoring various human real-time motions by the changes in the resistance. As shown in Fig. 7f, the resistance of the sensors changes correspondingly with the changes of the prosthetic finger bending angles, and the amplitude of the signal increases as the bending angle increases and vice versa [51]. Besides, other types of body movements could also be monitored sensitively like elbow and finger (Fig. 7g and h) [52]. Reported ionogel sensors rarely possess the combined good properties aforementioned, as displayed in Table S1.

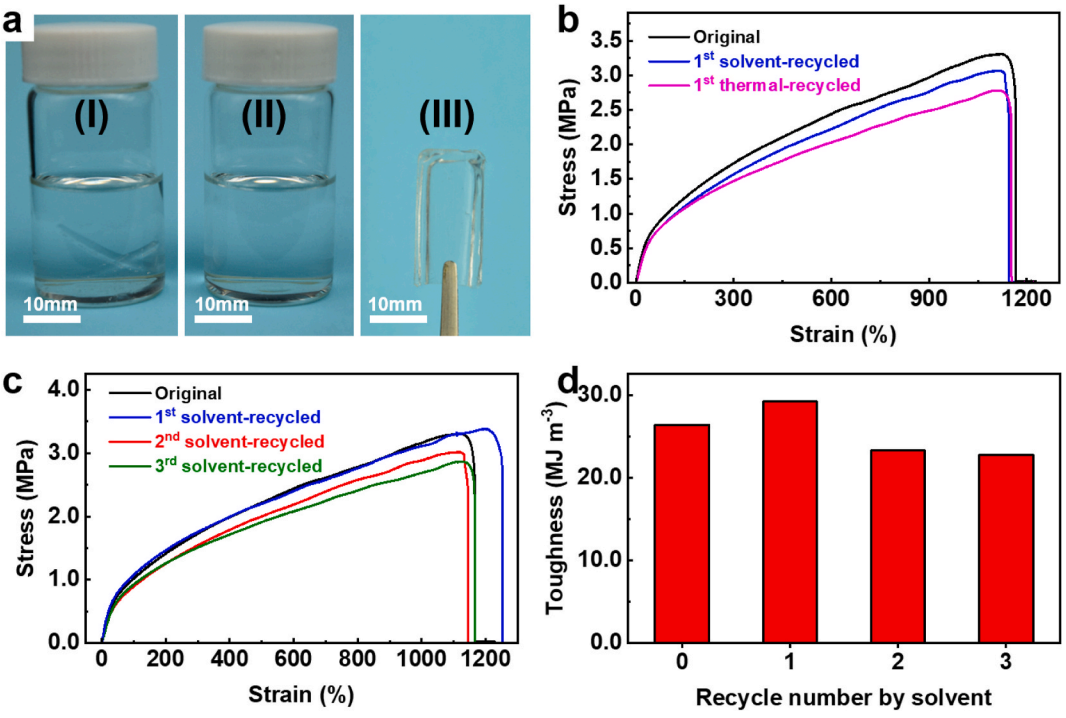

Fig. 6. Investigation of the recyclability of the scPLA-PEG/30%-ILs. (a) Photographs of the scPLA-PEG ionogels (I) soaked in THF, (II) dissolved in THF, and (III) solvent-recycled scPLA-PEG/30%-ILs film. (b) Tensile stress-strain curves of the original scPLA-PEG/30%-ILs and the first-time solvent- and thermal-recycled scPLA-PEG/30%-ILs. (c) Tensile stress-strain and (d) toughness curves of the original scPLA-PEG/30%-ILs and the solvent-recycled scPLA-PEG/30%-ILs with different recycle numbers, where the zero solvent recycle number corresponds to the original scPLA-PEG/30%-ILs without any solvent-recycle process.

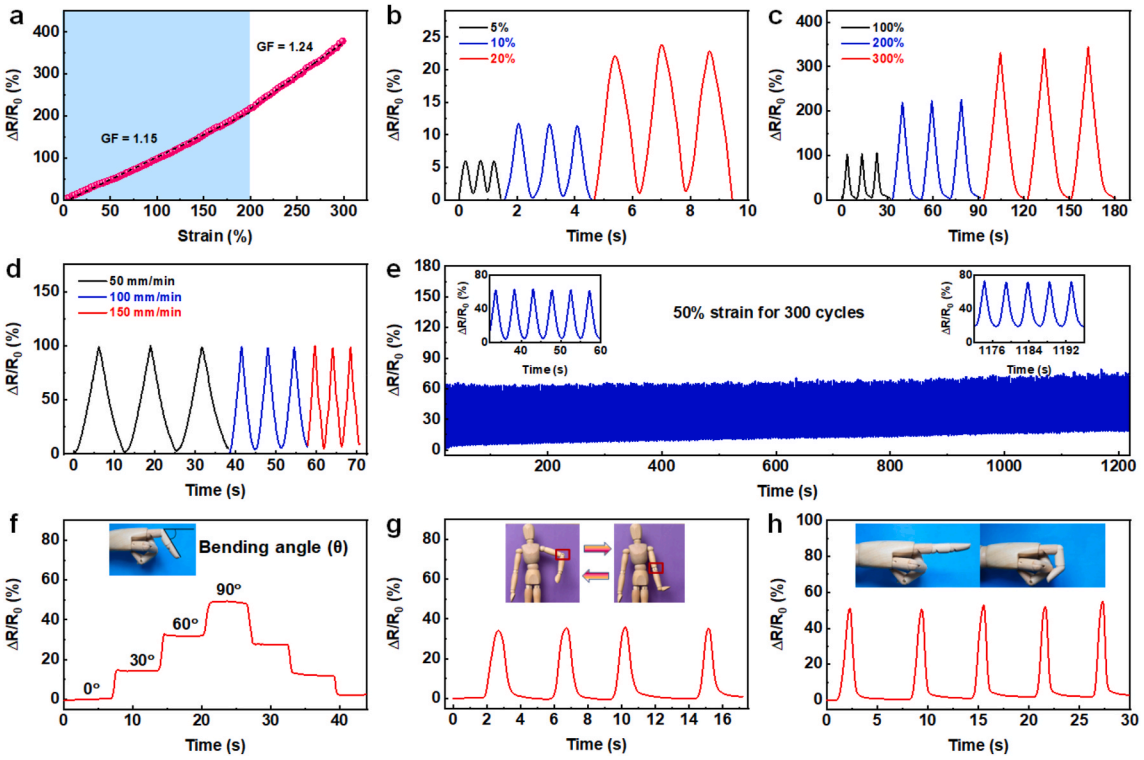

Fig. 7. (a) Relative resistance variations of as a function of strain. Relative resistance variations under (b) small (5%, 10%, and 20%) and (c) large (100%, 200%, and 300%) strain. (d) Relative resistance variations at loading rate upon stretching to 100% strain. (e) Cyclic stability tests under 50% strain for 300 cycles. Relative resistance variations of the sensors monitoring (f) finger bending under varied angle of bend and rapid changes in the (g) elbows and (h) fingers.

4. Conclusion

The unique structure of spider silk with the β-sheet nanocrystals consisting of hydrogen-bonded polypeptide chains cross-linked by the flexible chains creates new opportunities for designing materials with outstanding mechanical properties. Inspired by the biomolecular system of spider silk, we fabricated recyclable and biodegradable ionogels possessing the combinational properties of excellent mechanical strength, stretchability and elasticity via a novel yet simple strategy, and further demonstrated their use in flexible wearable sensors. The scaffold scPLA-PEG of the ionogels was synthesized from PLLA, PDLA and PEG. The formed scPLA-PEG possesses the spider-silk-like two-phase structure with hydrogen-bonded stereocomplex nanocrystals being cross-linked by flexible PEG chains, and displayed much higher mechanical properties than those of PLLA-PEG and PDLA-PEG counterparts. The scPLA-PEG ionogels also maintain the excellent elasticity at low temperature (−30 °C) and even at high temperature (70 °C). Importantly, the scPLA-PEG ionogels can be recycled and reshaped under a mild condition after being dissolved because of the reversibility of the stereocomplex nanocrystals cross-linkers. The assembled sensors based scPLA-PEG ionogels can be used as the highly sensitive flexible sensors to precisely detect various human motions (such as wrist, elbow, and finger bending). It could be envisioned that the present work presents a promising platform for the development of recyclable and biodegradable ionogels with superior properties, which are favorable for fabricating the next-generation flexible electronics and the realization of a sustainable society.

Author statement

Haopeng Zhang: Investigation, Methodology, Formal analysis, Data curation, Visualization, Writing – original draft. **Xiaohui Yu:** Data curation, Visualization. **Yufei Wang:** Formal analysis, Visualization. **Xiaoshan Fan**: Conceptualization, Investigation, Visualization, Writing – review & editing, Supervision, Funding acquisition. **Yue-E Miao:** Writing – review & editing, Supervision. **Xu Zhang:** Visualization, Writing – review & editing, Supervision, Funding acquisition. **Tianxi Liu:** Supervision, Funding acquisition.

Declaration of competing interest

The authors declare that they have no known competing financial interests or personal relationships that could have appeared to influence the work reported in this paper.

Data availability

The authors are unable or have chosen not to specify which data has been used.

Acknowledgements

This work was financially supported by the National Natural Science Foundation of China (52103074, 21875033, and 52161135302), the Research Foundation Flanders (G0F2322N), the Natural Science Foundation of Shanghai (21ZR1402800), and the Innovation Program of Shanghai Municipal Education Commission (2021-01-07-00-03-E00108).

Appendix A. Supplementary data

Supplementary data to this article can be found online at https://doi.org/10.1016/j.compscitech.2022.109740.

References

[1] M.S. Ganewatta, Z. Wang, C. Tang, Chemical syntheses of bioinspired and biomimetic polymers toward biobased materials, Nat. Rev. Chem 5 (11) (2021) 753–772, https://doi.org/10.1038/s41570-021-00325-x.

[2] S. Keten, M.J. Buehler, Geometric confinement governs the rupture strength of H-bond assemblies at a critical length scale, Nano Lett. 8 (2) (2008) 743–748.

[3] J.C. Johnson, N.D. Wanasekara, L.T. Korley, Utilizing peptidic ordering in the design of hierarchical polyurethane/ureas, Biomacromolecules 13 (5) (2012) 1279–1286, https://doi.org/10.1021/bm201800v.

[4] S. Yu, R. Zhang, Q. Wu, T. Chen, P. Sun, Bio-inspired high-performance and recyclable cross-linked polymers, Adv. Mater. 25 (35) (2013) 4912–4917, https://doi.org/10.1002/adma.201301513.

[5] Y. Song, Y. Liu, T. Qi, G.L. Li, Towards dynamic but supertough healable polymers through biomimetic hierarchical hydrogen-bonding interactions, Angew Chem. Int. Ed. Engl. 57 (42) (2018) 13838–13842, https://doi.org/10.1002/anie.201807622.

[6] Z. Li, Y.L. Zhu, W. Niu, X. Yang, Z. Jiang, Z.Y. Lu, X. Liu, J. Sun, Healable and recyclable elastomers with record-high mechanical robustness, unprecedented crack tolerance, and superhigh elastic restorability, Adv. Mater. 33 (27) (2021), 2101498, https://doi.org/10.1002/adma.202101498.

[7] L. Gu, Y. Jiang, J. Hu, Scalable spider-silk-like supertough fibers using a pseudoprotein polymer, Adv. Mater. 31 (48) (2019), 1904311, https://doi.org/10.1002/adma.201904311.

[8] F. Wang, Z. Yang, J. Li, C. Zhang, P. Sun, Bioinspired polyurethane using multifunctional block modules with synergistic dynamic bonds, ACS Macro Lett. 10 (5) (2021) 510–517, https://doi.org/10.1021/acsmacrolett.1c00054.

[9] G. Xu, Q. Wang, Chemically recyclable polymer materials: polymerization and depolymerization cycles, Green Chem. 24 (6) (2022) 2321–2346, https://doi.org/10.1039/d1gc03901f.

[10] R. Yang, G. Xu, B. Dong, H. Hou, Q. Wang, A "Polymer to polymer'' chemical recycling of PLA plastics by the "DE-RE polymerization'' strategy, Macromolecules 55 (5) (2022) 1726–1735, https://doi.org/10.1021/acs.macromol.1c02085.

[11] H. Dinh Xuan, B. Timothy, H.Y. Park, T.N. Lam, D. Kim, Y. Go, J. Kim, Y. Lee, S. I. Ahn, S.H. Jin, J. Yoon, Super stretchable and durable electroluminescent devices based on double-network ionogels, Adv. Mater. 33 (25) (2021), 2008849, https://doi.org/10.1002/adma.202008849.

[12] H. Li, F. Xu, T. Guan, Y. Li, J. Sun, Mechanically and environmentally stable triboelectric nanogenerator based on high-strength and anti-compression self-healing ionogel, Nano Energy 90 (2021), 106645, https://doi.org/10.1016/j.nanoen.2021.106645.

[13] N. Bai, L. Wang, Q. Wang, J. Deng, Y. Wang, P. Lu, J. Huang, G. Li, Y. Zhang, J. Yang, K. Xie, X. Zhao, C.F. Guo, Graded intrafillable architecture-based iontronic pressure sensor with ultra-broad-range high sensitivity, Nat. Commun. 11 (1) (2020) 209, https://doi.org/10.1038/s41467-019-14054-9.

[14] E. Kamio, T. Yasui, Y. Iida, J.P. Gong, H. Matsuyama, Inorganic/organic double-network gels containing ionic liquids, Adv. Mater. 29 (47) (2017), 201704118, https://doi.org/10.1002/adma.201704118.

[15] Y. Ren, Z. Liu, G. Jin, M. Yang, Y. Shao, W. Li, Y. Wu, L. Liu, F. Yan, Electric-field-induced gradient ionogels for highly sensitive, broad-range-response, and freeze/heat-resistant ionic fingers, Adv. Mater. 33 (12) (2021), 2008486, https://doi.org/10.1002/adma.202008486.

[16] N. Jiang, H. Li, D. Hu, Y. Xu, Y. Hu, Y. Zhu, X. Han, G. Zhao, J. Chen, X. Chang, M. Xi, Q. Yuan, Stretchable strain and temperature sensor based on fibrous polyurethane film saturated with ionic liquid, Compos. Commun. 27 (2021), 100845, https://doi.org/10.1016/j.coco.2021.100845.

[17] X. Yu, H. Zhang, Y. Wang, X. Fan, Z. Li, X. Zhang, T. Liu, Highly stretchable, ultra-soft, and fast self-healable conductive hydrogels based on polyaniline nanoparticles for sensitive flexible sensors, Adv. Funct. Mater. (2022), 2204366, https://doi.org/10.1002/adfm.202204366.

[18] J. Ruiz-Olles, P. Slavik, N.K. Whitelaw, D.K. Smith, Self-assembled gels formed in deep eutectic solvents: supramolecular eutectogels with high ionic conductivity, Angew Chem. Int. Ed. Engl. 58 (13) (2019) 4173–4178, https://doi.org/10.1002/anie.201810600.

[19] L. Shi, K. Jia, Y. Gao, H. Yang, Y. Ma, S. Lu, G. Gao, H. Bu, T. Lu, S. Ding, Highly stretchable and transparent ionic conductor with novel hydrophobicity and extreme-temperature tolerance, Research 2020 (2020), 2505619, https://doi.org/10.34133/2020/2505619.

[20] T. Li, Y. Wang, S. Li, X. Liu, J. Sun, Mechanically robust, elastic, and healable ionogels for highly sensitive ultra-durable ionic skins, Adv. Mater. 32 (32) (2020), 2002706, https://doi.org/10.1002/adma.202002706.

[21] L. Wang, Y. Wang, S. Yang, X. Tao, Y. Zi, W.A. Daoud, Solvent-free adhesive ionic elastomer for multifunctional stretchable electronics, Nano Energy 91 (2022), 106611, https://doi.org/10.1016/j.nanoen.2021.106611.

[22] Y. Zhong, G.T.M. Nguyen, C. Plesse, F. Vidal, E.W.H. Jager, Tailorable, 3D structured and micro-patternable ionogels for flexible and stretchable electrochemical devices, J. Mater. Chem. C 7 (2) (2019) 256–266, https://doi.org/10.1039/c8tc04368j.

[23] P. Shi, Y. Wang, K. Wan, C. Zhang, T. Liu, A waterproof ion-conducting fluorinated elastomer with 6000% stretchability, superior ionic conductivity, and harsh environment tolerance, Adv. Funct. Mater. 32 (22) (2022), 2112293, https://doi.org/10.1002/adfm.202112293.

[24] J. Duan, W. Xie, P. Yang, J. Li, G. Xue, Q. Chen, B. Yu, R. Liu, J. Zhou, Tough hydrogel diodes with tunable interfacial adhesion for safe and durable wearable batteries, Nano Energy 48 (2018) 569–574, https://doi.org/10.1016/j.nanoen.2018.04.014.

[25] L. Xu, Z. Huang, Z. Deng, Z. Du, T.L. Sun, Z.H. Guo, K. Yue, A transparent, highly stretchable, solvent-resistant, recyclable multifunctional ionogel with underwater self-healing and adhesion for reliable strain sensors, Adv. Mater. 33 (51) (2021), 2105306, https://doi.org/10.1002/adma.202105306.

[26] D.G. Seo, H.C. Moon, Mechanically robust, highly ionic conductive gels based on random copolymers for bending durable electrochemical devices, Adv. Funct. Mater. 28 (14) (2018), 1706948, https://doi.org/10.1002/adfm.201706948.

[27] J. Wei, Y. Zheng, T. Chen, A fully hydrophobic ionogel enables highly efficient wearable underwater sensors and communicators, Mater. Horiz. 8 (10) (2021) 2761–2770, https://doi.org/10.1039/d1mh00998b.

[28] B. Qin, S. Zhang, P. Sun, B. Tang, Z. Yin, X. Cao, Q. Chen, J.F. Xu, X. Zhang, Tough and multi-recyclable cross-linked supramolecular polyureas via incorporating noncovalent bonds into main-chains, Adv. Mater. 32 (36) (2020), 2000096, https://doi.org/10.1002/adma.202000096.

[29] Z. Zhou, C. Qian, W. Yuan, Self-healing, anti-freezing, adhesive and remoldable hydrogel sensor with ion-liquid metal dual conductivity for biomimetic skin, Compos. Sci. Technol. 203 (2021), https://doi.org/10.1016/j.compscitech.2020.108608.

[30] W.-Q. Yuan, G.-L. Liu, C. Huang, Y.-D. Li, J.-B. Zeng, Highly stretchable, recyclable, and fast room temperature self-healable biobased elastomers using polycondensation, Macromolecules 53 (22) (2020) 9847–9858, https://doi.org/10.1021/acs.macromol.0c01665.

[31] C.-J. Fan, Z.-B. Wen, Z.-Y. Xu, Y. Xiao, D. Wu, K.-K. Yang, Y.-Z. Wang, Adaptable strategy to fabricate self-healable and reprocessable poly(thiourethane-urethane) elastomers via reversible thiol–isocyanate click chemistry, Macromolecules 53 (11) (2020) 4284–4293, https://doi.org/10.1021/acs.macromol.0c00239.

[32] X. Ming, L. Shi, H. Zhu, Q. Zhang, Stretchable, phase-transformable ionogels with reversible ionic conductor-insulator transition, Adv. Funct. Mater. 30 (49) (2020), 2005079, https://doi.org/10.1002/adfm.202005079.

[33] L. Shi, T. Zhu, G. Gao, X. Zhang, W. Wei, W. Liu, S. Ding, Highly stretchable and transparent ionic conducting elastomers, Nat. Commun. 9 (1) (2018) 2630, https://doi.org/10.1038/s41467-018-05165-w.

[34] X. Liu, Q. Zhang, L. Duan, G. Gao, Bioinspired nucleobase-driven nonswellable adhesive and tough gel with excellent underwater adhesion, ACS Appl. Mater. Interfaces 11 (6) (2019) 6644–6651, https://doi.org/10.1021/acsami.8b21686.

[35] X. Yu, Y. Zheng, Y. Wang, H. Zhang, H. Song, Z. Li, X. Fan, T. Liu, Facile fabrication of highly stretchable, stable, and self-healing ion-conductive sensors for monitoring human motions, Chem. Mater. 34 (3) (2022) 1110–1120, https://doi.org/10.1021/acs.chemmater.1c03547.

[36] Z. Li, J.K. Muiruri, W. Thitsartarn, X. Zhang, B.H. Tan, C. He, Biodegradable silica rubber core-shell nanoparticles and their stereocomplex for efficient PLA toughening, Compos. Sci. Technol. 159 (2018) 11–17, https://doi.org/10.1016/j.compscitech.2018.02.026.

[37] Z. Li, B.H. Tan, T. Lin, C. He, Recent advances in stereocomplexation of enantiomeric PLA-based copolymers and applications, Prog. Polym. Sci. 62 (2016) 22–72, https://doi.org/10.1016/j.progpolymsci.2016.05.003.

[38] B.H. Tan, J.K. Muiruri, Z. Li, C. He, Recent progress in using stereocomplexation for enhancement of thermal and mechanical property of polylactide, ACS Sustain. Chem. Eng. 4 (10) (2016) 5370–5391, https://doi.org/10.1021/acssuschemeng.6b01713.

[39] X. Fan, B.H. Tan, Z. Li, X.J. Loh, Control of PLA stereoisomers-based polyurethane elastomers as highly efficient shape memory materials, ACS Sustain. Chem. Eng. 5 (1) (2016) 1217–1227, https://doi.org/10.1021/acssuschemeng.6b02652.

[40] Y. Lyu, X. Wen, G. Wang, Q. Zhang, L. Lin, A.K. Schlarb, X. Shi, 3D printing nanocomposites with controllable "strength-toughness" transition: modification of SiO2 and construction of Stereocomplex Crystallites, Compos. Sci. Technol. 218 (2022), https://doi.org/10.1016/j.compscitech.2021.109167.

[41] L. Mei, Y. Ren, Y. Gu, X. Li, C. Wang, Y. Du, R. Fan, X. Gao, H. Chen, A. Tong, L. Zhou, G. Guo, Strengthened and thermally resistant poly(lactic acid)-based composite nanofibers prepared via easy stereocomplexation with antibacterial effects, ACS Appl. Mater. Interfaces 10 (49) (2018) 42992–43002, https://doi.org/10.1021/acsami.8b14841.

[42] B. Ma, H. Zhang, K. Wang, H. Xu, Y. He, X. Wang, Influence of scPLA microsphere on the crystallization behavior of PLLA/PDLA composites, Compos. Commun. 21 (2020), 100380, https://doi.org/10.1016/j.coco.2020.100380.

[43] V. Izraylit, P.J. Hommes-Schattmann, A.T. Neffe, O.E.C. Gould, A. Lendlein, Polyester urethane functionalizable through maleimide side-chains and cross-linkable by polylactide stereocomplexes, Eur. Polym. J. 137 (2020), 109916, https://doi.org/10.1016/j.eurpolymj.2020.109916.

[44] V. Izraylit, O.E.C. Gould, T. Rudolph, K. Kratz, A. Lendlein, Controlling actuation performance in physically cross-linked polylactone blends using polylactide stereocomplexation, Biomacromolecules 21 (2) (2020) 338–348, https://doi.org/10.1021/acs.biomac.9b01279.

[45] X. Zhou, B. Guo, L. Zhang, G.H. Hu, Progress in bio-inspired sacrificial bonds in artificial polymeric materials, Chem. Soc. Rev. 46 (20) (2017) 6301–6329, https://doi.org/10.1039/c7cs00276a.

[46] Q. Xia, S. Wang, W. Zhai, C. Shao, L. Xu, D. Yan, N. Yang, K. Dai, C. Liu, C. Shen, Highly linear and low hysteresis porous strain sensor for wearable electronic skins, Compos. Commun. 26 (2021), 100809, https://doi.org/10.1016/j.coco.2021.100809.

[47] C. Fan, D. Wang, J. Huang, H. Ke, Q. Wei, A highly sensitive epidermal sensor based on triple-bonded hydrogels for strain/pressure sensing, Compos. Commun. 28 (2021), 100951, https://doi.org/10.1016/j.coco.2021.100951.

[48] Y. Fang, H. Cheng, H. He, S. Wang, J. Li, S. Yue, L. Zhang, Z. Du, J. Ouyang, Stretchable and transparent ionogels with high thermoelectric properties, Adv.

Funct. Mater. 30 (51) (2020), 2004699, https://doi.org/10.1002/adfm.202004699.
[49] Y. Guo, L. Yang, L. Zhang, S. Chen, L. Sun, S. Gu, Z. You, A dynamically hybrid crosslinked elastomer for room-temperature recyclable flexible electronic devices, Adv. Funct. Mater. 31 (50) (2021), 2106281, https://doi.org/10.1002/adfm.202106281.
[50] M. Yue, Y. Wang, H. Guo, C. Zhang, T. Liu, 3D reactive printing of polyaniline hybrid hydrogel microlattices with large stretchability and high fatigue resistance for wearable pressure sensors, Compos. Sci. Technol. 220 (2022), https://doi.org/10.1016/j.compscitech.2022.109263.
[51] R. Hu, G. Ji, J. Zhao, X. Gu, L. Zhou, J. Zheng, The preparation of dual cross-linked high strain composite gel with manifold excellent properties and its application as a strain sensor, Compos. Sci. Technol. 217 (2022), https://doi.org/10.1016/j.compscitech.2021.109110.
[52] Y. Xu, Q. Feng, C. Zhang, T. Liu, Wet-spinning of ionic liquid@elastomer coaxial fibers with high stretchability and wide temperature resistance for strain sensors, Compos. Commun. 25 (2021), 100693, https://doi.org/10.1016/j.coco.2021.100693.